

Nanoscale metal–semiconductor–metal photodetectors with subpicosecond response time fabricated using electron beam lithography

M. Y. Liu and S. Y. Chou

Department of Electrical Engineering, University of Minnesota, Minneapolis, Minnesota 55455

T. Y. Hsiang, S. Alexandrou, and R. Sobolewski

Department of Electrical Engineering, University of Rochester, Rochester, New York 14627

(Received 27 May 1992; accepted 24 July 1992)

Metal–semiconductor–metal photodetectors (MSM PDs) with finger spacing and width as small as 25 nm have been fabricated using high-resolution electron beam lithography. Measurements using an electro-optic sampling system show that the fastest detector has a full width at half-maximum response time of 0.87 ps and a 3 dB bandwidth of 510 GHz. Monte Carlo simulation of detector response time is studied and compared with experimental data. Finally, scaling rules for high-speed MSM PDs are proposed.

I. INTRODUCTION

Recently, much progress has been made in high-speed metal–semiconductor–metal photodetectors (MSM PDs), since they are very attractive for optical communication, future high-speed chip-to-chip connection, and high-speed sampling.^{1–9} MSM PDs can be classified according to whether their speed is intrinsically limited by the carrier transit time between the fingers or the carrier recombination time. Certainly, the speed of the detectors will be limited by the $R-C$ time constant if it is larger than the transit time or the recombination time. Usually, transit-time-limited detectors are fabricated on high-quality semiconductors and have a sensitivity several orders of magnitude higher than that of recombination-time-limited MSM PDs. However, in the past, the transit-time-limited MSM PDs generally were much slower than the recombination-time-limited MSM PDs, because it was difficult to fabricate small fingers.

As fabrication technology advances, the finger spacing of a MSM PD can be reduced to nanometer scale. The smaller the finger spacing, the shorter the intrinsic response time for the transit-time-limited MSM PDs, and the higher the sensitivity for the recombination-time-limited MSM PDs. Therefore, the difference in speed and sensitivity between the transit-time-limited and recombination-time-limited MSM PDs is getting smaller. Furthermore, the finger width is another important factor for high-speed MSM PDs. The narrower the finger width, the less the detector capacitance and the shorter the external response time.

Previously, the fastest transit-time-limited GaAs MSM PD reported has a finger width of 0.75 μm and finger spacing of 0.5 μm , an impulse response of 4.8 ps full width at half-maximum (FWHM), and a 3 dB bandwidth of 105 GHz.⁴ The fastest recombination-time-limited MSM PD on low-temperature (LT) grown GaAs reported previously had a finger width and spacing of 0.2 μm , a FWHM of 1.2 ps, and a 3 dB bandwidth of 375 GHz.⁶ The fastest MSM PD on crystalline silicon reported previously had a 4 μm single gap and a 3 dB bandwidth of 22 GHz.⁷

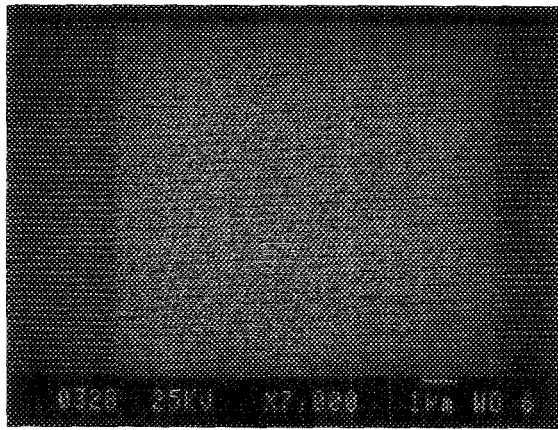
In this article, the fabrication of MSM PDs with finger

spacing and width as small as 25 nm on bulk and LT GaAs, and crystalline Si is reported. Monte Carlo simulation of the impulse response of nanoscale MSM PDs and scaling rules for high-speed MSM PDs is presented. Finally, the subpicosecond characterization of the nanoscale MSM PDs is reported.

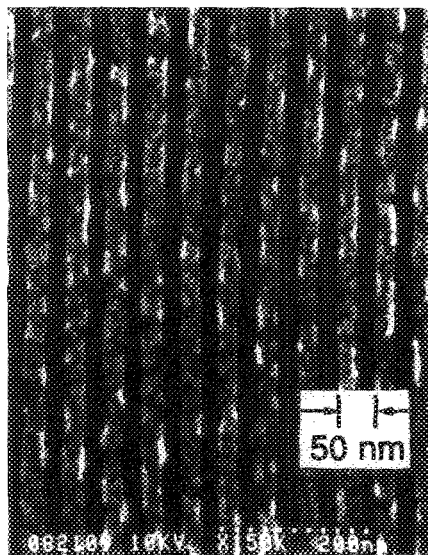
II. FABRICATION

Three different substrates were studied: bulk GaAs, LT GaAs, and crystalline silicon. The bulk GaAs substrate is semi-insulating (SI) GaAs with a carrier concentration of $\sim 1.5 \times 10^7 \text{ cm}^{-3}$, electron mobility of 6500 $\text{cm}^2/\text{V s}$, and resistivity of $5 \times 10^7 \Omega \text{ cm}$. The LT GaAs was 1 μm thick and grown at 210 $^\circ\text{C}$ and annealed at 600 $^\circ\text{C}$ for 1 h. The Si substrate was p -type with a doping concentration of $8 \times 10^{14} \text{ cm}^{-3}$.

For high-speed measurements, the detectors were fabricated with coplanar striplines of Ti/Au (50 nm/200 nm thick) with a linewidth of 16 μm , a spacing of 9 μm , and a characteristic impedance of 75 Ω . The transmission lines and alignment marks for electron beam lithography (EBL) were defined using photolithography and lift-off. The nanoscale MSM PDs were fabricated using EBL and a lift-off technique. The fabrication steps consist of electron beam resist coating, direct electron beam writing, development, metal evaporation, and a lift-off process. First, polymethylmethacrylate (PMMA) was spun on the substrate. For MSM PDs with finger pitch smaller than 200 nm, a single layer PMMA with thickness from 40 to 70 nm was used; for finger pitch greater than 200 nm, double layer PMMA was used, with a 70 nm thick layer of 100 K molecular weight PMMA on the bottom, and a 70 nm thick layer of 950 K molecular weight PMMA on the top. The double layer scheme is designed to achieve undercut in the resist for easier lift-off. Each layer of PMMA was baked at 160 $^\circ\text{C}$ for over 12 h after spinning. Interdigitated line patterns were exposed in the resist using a custom-built high-resolution EBL system converted from a JEOL-840 scanning electron microscope operated at 35 kV.¹⁰ The exposed PMMA was developed in 2-Ethoxyethanol:methanol (3:7 by volume). After exposure and develop-



(a)



(b)

FIG. 1. Scanning electron micrographs of MSM PDs of (a) 50 nm finger spacing and 50 nm finger width, and (b) 25 nm spacing and 25 nm width. The metals are Ti/Au.

ment, metals (Ti/Au) were evaporated onto the samples and were lifted-off in acetone. The total metal thickness is from 15 to 30 nm for single layer resist and 50 nm for double layer resist, respectively. Figure 1 shows scanning electron micrographs of (a) MSM PDs of 50 nm finger spacing and width and a detection area of $10 \mu\text{m} \times 10 \mu\text{m}$, and (b) MSM PD with finger spacing and width of 25 nm.

III. MODELING AND SCALING

A Monte Carlo simulation program has been developed for simulating the intrinsic impulse response of transit-time-limited MSM PDs.⁹ Figure 2 shows the intrinsic response time versus the finger spacing of transit-time-limited MSM PDs on GaAs and Si. Although the response time of a Si MSM PD is longer than that of GaAs, due to the heavier electron effective mass, the intrinsic response time of a Si MSM PD with a 25 nm finger spacing can reach 1 ps and the 3 dB bandwidth can be 450 GHz (excluding hole current), very promising for application in Si-based optoelectronics. In the simulation, it was assumed

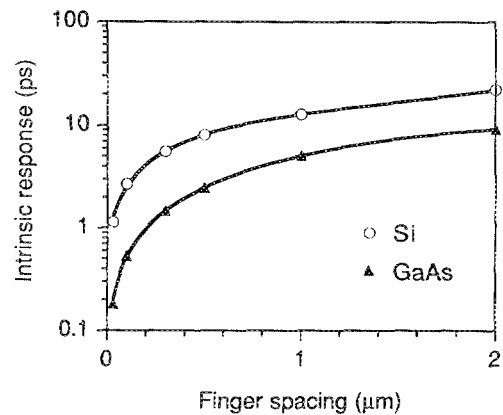


FIG. 2. The calculated intrinsic response time vs finger spacing on GaAs and Si MSM PDs.

that the maximum velocity of carriers is the saturation velocity, $2 \times 10^7 \text{ cm/s}$ for GaAs and $1 \times 10^7 \text{ cm/s}$ for Si. This certainly can be an underestimation for the MSM PDs of sub-100 nm finger spacing, because of electron velocity overshoot. This fast device operation due to carrier velocity overshoot is a unique feature of nanoscale MSM PDs.

Parasitic capacitance of a MSM PD can be a limiting factor to its speed. Detector's capacitance was calculated using conformal mapping.¹¹ For a given detector area and finger pitch size, the smaller the finger width, the smaller the detector's capacitance. When the finger width is very narrow, however, the series resistance of metal fingers may become comparable to the load resistance and therefore increase R - C time constant. Nanoscale metal lines on SiO_2 substrate were fabricated and their resistances were measured.⁸ The thin metal line resistance is greater than that calculated from bulk resistance due to metal surface scattering. The total series resistance of a detector were therefore calculated from the measured line resistances and its geometry.

Based on the simulation and the calculation of detector's capacitance and series resistance, general scaling rules

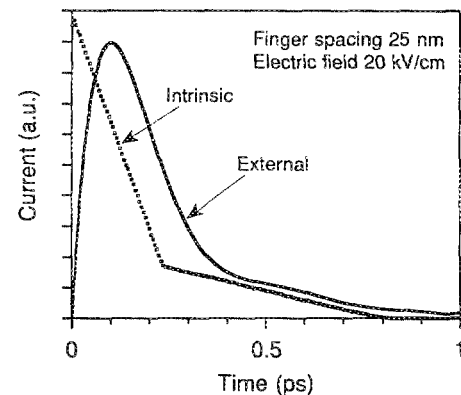


FIG. 3. Calculated intrinsic and external impulse responses of a GaAs MSM PD with 25 nm finger spacing and width. The detector total area is $1 \mu\text{m} \times 1 \mu\text{m}$. The detector capacitance of 1.2 fF and the load resistance of 50Ω were used to calculate the external response.

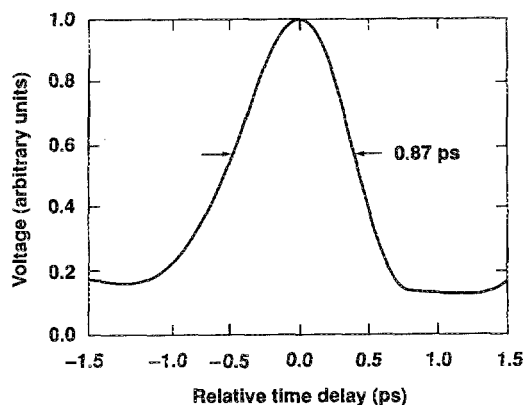


FIG. 4. Response of a LT GaAs MSM PD with 300 nm finger spacing and width at 1.5 V bias.

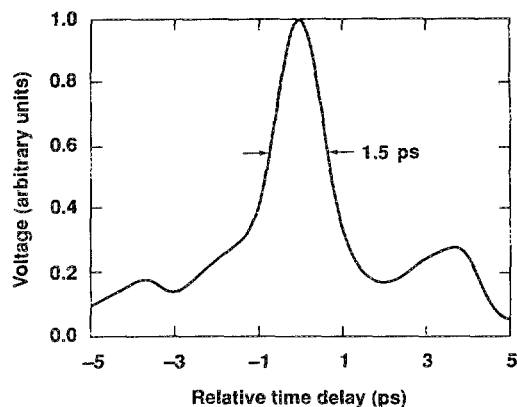


FIG. 5. Response of a bulk GaAs MSM PD with 100 nm finger spacing and width at 1.5 V bias.

for designing high-speed MSM PDs can be summarized. (1) For decreasing the intrinsic response time of transit-time-limited MSM PDs, the finger spacing should be reduced. (2) For reducing the MSM PD's capacitance, the ratio of finger width to finger spacing and/or detector's active area have to be reduced. (3) For cutting off the tails in the impulse response of MSM PDs, the hole current must be reduced or eliminated. And (4) for reducing metal finger resistance, it is preferable to use shorter fingers and thicker metal.

According to the scaling rules and the fabrication capability, the intrinsic and external impulse responses of a GaAs MSM PD with 25 nm finger spacing and width and $1 \mu\text{m} \times 1 \mu\text{m}$ area (Fig. 3) was simulated. The detector capacitance is 1.2 fF. It was assumed that the load resistance is 50Ω , the series resistance is not important since it is smaller than the load resistance.⁸ The FWHM intrinsic response time of the detector is 0.16 ps, and the FWHM external response time is 0.25 ps. The current peak in the response is due to electrons and the long tail is due to holes that move much slower than the electrons. Fourier transforms of the external responses with and without hole current show that the detector's 3 dB bandwidth is 400 GHz, and when the hole current is eliminated, 3 dB bandwidth is over 1.8 THz.

IV. EXPERIMENTAL RESULTS

High-speed measurement was performed using an electro-optic sampling system consisting of a 100 fs colliding-pulse mode-locked dye laser with a wavelength of 620 nm and a repetition rate of 100 MHz.¹² The 100 fs laser pulse is splitted into two: one for exciting the MSM

PDs and the other for sampling the electrical signal generated by the exciting pulse. The sampling utilizes the Pockel effect in LiTaO₃ tip placed 250 μm from the detectors. By changing the relative delay between the exciting pulse and the sampling pulse, the response of a MSM PD can be mapped out.

MSM PDs on LT GaAs with different finger spacings and widths, 100, 200, and 300 nm, were tested. The 300 nm detector has a FWHM of 0.87 ps (Fig. 4) and 3 dB bandwidth of 510 GHz. The impulse response time of the PDs becomes progressively worse as the finger spacing and width become smaller. The calculated intrinsic transit time, R - C time constant, measured FWHM, and 3 dB bandwidth of these detectors was tabulated in Table I. The R - C time constant is the product of the calculated detector capacitance and the impedance of the transmission line (75Ω). The resistance of metal fingers is not important in this case because it is smaller than the transmission line impedance. As shown in Table I, for the 300 nm LT GaAs MSM PD, the measured FWHM is shorter than the intrinsic transit time, but longer than R - C time constant; therefore, its speed is dominated by the carrier recombination time of the LT GaAs. On the other hand, for LT GaAs MSM PDs with finger spacing and width of 100 and 200 nm, the measured FWHM responses are longer than 0.87 ps and the intrinsic transit time, but comparable to the calculated 0.67 R - C constants. This implies that they are limited by the R - C time constant.

A MSM PD on bulk GaAs with 100 nm finger spacing and width was also tested. The impulse response has a FWHM of 1.5 ps (Fig. 5) and 3 dB bandwidth of 300 GHz. The fact that this MSM has almost the same re-

TABLE I. Theoretical and experimental data of MSM PDs with different structures on LT GaAs, bulk GaAs, and Si.

Semiconductor	LT GaAs			Bulk GaAs	Bulk Si
Finger spacing/width (nm)	100/100	200/200	300/300	100/100	100/100
Intrinsic transit time (ps)	0.4	0.8	1.1	0.4	2.7
R - C (ln2) time constant (ps)	1.56	1.04	0.52	1.56	1.56
Measured response (ps)	1.6	1.0	0.87	1.5	10.7
Measured bandwidth (GHz)	280	440	510	300	41

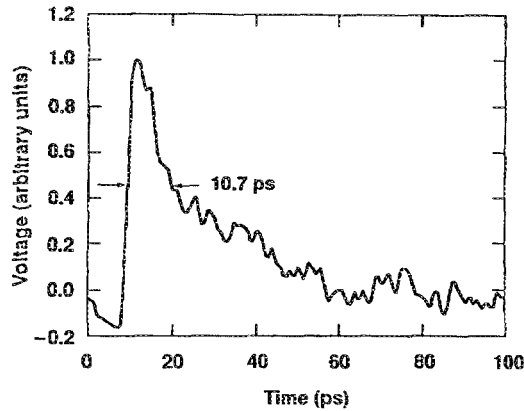


FIG. 6. Response of a Si MSM PD with 100 nm finger spacing and width at 1 V bias.

sponse time as that on LT GaAs with the same device dimension indicates that the speed of this 100 nm MSM PD on bulk GaAs is limited by the $R-C$ time.

Impulse response of a Si MSM PD with 100 nm finger spacing and width is shown in Fig. 6. The FWHM is 10.7 ps and the 3 dB bandwidth is 41 GHz. The response time of the Si detector is much longer than the estimated $R-C$ time and the transit time. It is suspected that this is either due to leakage current since the active region is not isolated and the laser beam may illuminate the area outside the detector, or due to diffusion current from the carriers generated deep inside the semiconductor since the light absorption length of Si is $\sim 3 \mu\text{m}$. Investigation is still in process. Nonetheless, to our knowledge, this is the fastest MSM PD on crystalline Si ever reported.

V. SUMMARY

In summary, using a custom-built EBL system, MSM PDs with finger spacing and width as small as 25 nm on

several semiconductor substrates were fabricated. Subpicosecond characterization using electro-optic sampling showed that the fastest MSM PDs had FWHM response times and 3 dB bandwidths, respectively, of 0.87 ps and 510 GHz on LT GaAs; 1.5 ps and 300 GHz on bulk GaAs; and 10.7 ps and 40 GHz on bulk Si. Based on Monte Carlo simulation, calculation of capacitance and resistance, and experimental data, scaling rules for achieving high-speed MSM PDs were proposed.

ACKNOWLEDGMENTS

The work at the University of Minnesota was partially supported by the Packard Foundation, IBM, ARO, NSF, and SRC. The work at the University of Rochester was supported by the sponsors of the Laser Fusion Feasibility Project at the Laboratory for Laser Energetics.

- ¹M. Ito and O. Wada, *IEEE J. Quantum Electron.* **QE-22**, 1073 (1986).
- ²G. K. Chang, H. Schumacher, R. F. Leheny, P. Gerskovich, and S. Nelson, *IEEE GaAs IC Symposium*, Portland, Oregon, Oct. 1987 (unpublished), pp. 57–60.
- ³C. S. Harder, B. van Zeghbroeck, H. Meier, W. Patrick, and P. Vettiger, *IEEE Electron. Device Lett.* **EDL-9**, 171 (1988).
- ⁴B. J. van Zeghbroeck, W. Patrick, J. M. Halbout, and P. Vettiger, *IEEE Electron. Device Lett.* **EDL-9**, 527 (1988).
- ⁵K. Nakajima, T. Iida, K. I. Sugimoto, H. Kan, and Y. Mizushima, *IEEE Trans. Electron Devices* **ED-37**, 31 (1990).
- ⁶Y. Chen, S. Williamson, T. Brock, F. W. Smith, and A. R. Calawa, *Appl. Phys. Lett.* **59**, 1984 (1991).
- ⁷B. W. Mullins, S. F. Soares, K. A. McArdle, C. W. Wilson, and S. R. J. Brueck, *IEEE Photon. Technol. Lett.* **3**, 360 (1991).
- ⁸S. Y. Chou, Y. Liu, and P. B. Fischer, *J. Vac. Sci. Technol. B* **9**, 2920 (1991).
- ⁹S. Y. Chou, Y. Liu, and P. B. Fischer, *Appl. Phys. Lett.* **61**, 477 (1992).
- ¹⁰S. Y. Chou and P. B. Fischer, *J. Vac. Sci. Technol. B* **8**, 1919 (1990).
- ¹¹Y. C. Lim and R. A. Moore, *IEEE Trans. Electron Devices* **ED-15**, 173 (1968).
- ¹²T. Y. Hsiang, S. Alexandrou, C. C. Wang, R. Sobolewski, S. Y. Chou, and Y. Liu, *Conference on Lasers and Electro-Optics*, Anaheim, CA, May 1992 (unpublished), paper JFD5.